Spectroscopic Characterization of the Metal-Binding Sites in the Periplasmic Metal-Sensor Domain of CnrX from Cupriavidus metallidurans CH34

9 AUTHORS, INCLUDING:

Isabelle Petit-Haertlein
Institut de Biologie Structurale (IBS)
29 PUBLICATIONS **453** CITATIONS

SEE PROFILE

Antoine Maillard
Institut de Biologie Structurale (IBS)
18 PUBLICATIONS **349** CITATIONS

SEE PROFILE

Anne Imberty
French National Centre for Scientific Research
361 PUBLICATIONS **10,380** CITATIONS

SEE PROFILE

Olivier Proux
French National Centre for Scientific Research
132 PUBLICATIONS **2,095** CITATIONS

SEE PROFILE

BIOCHEMISTRY
including biophysical chemistry & molecular biology

Article

pubs.acs.org/biochemistry

Spectroscopic Characterization of the Metal-Binding Sites in the Periplasmic Metal-Sensor Domain of CnrX from *Cupriavidus metallidurans* CH34

Juliette Trepreau,[†] Eve de Rosny,[†] Carole Duboc,[‡] Géraldine Sarret,[§] Isabelle Petit-Hartlein,[†] Antoine P. Maillard,[†] Anne Imberty,[‖] Olivier Proux,[⊥] and Jacques Covès*,[†]

[†]Institut de Biologie Structurale-Jean-Pierre Ebel, UMR 5075, CNRS-CEA-UJF-Grenoble-1, 41, rue Jules Horowitz, 38027 Grenoble Cedex, France

[‡]Département de Chimie Moléculaire, UMR-5250, Université Joseph Fourier Grenoble 1/CNRS, 38041 Grenoble Cedex 9 France

[§]Environmental Geochemistry Group, LGIT, University of Grenoble and CNRS, BP 53, 38041 Grenoble, Cedex 9, France

[‖]Centre de Recherche sur les Macromolécules Végétales - CNRS, 38041 Grenoble cedex 9, France

[⊥]CRG-FAME Beamline, European Synchrotron Radiation Facility, F-38043 Grenoble, France

Ⓢ *Supporting Information*
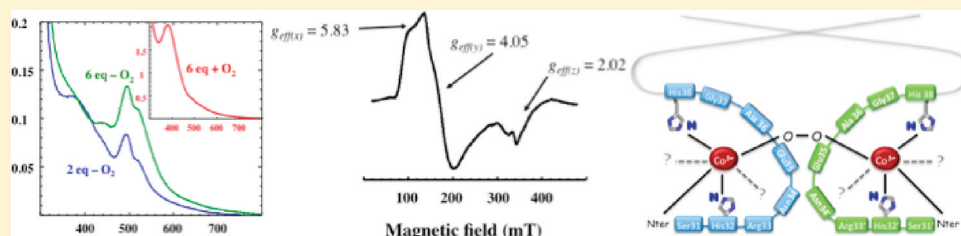
ABSTRACT: CnrX, the dimeric metal sensor of the three-protein transmembrane signal transduction complex CnrYXH of *Cupriavidus metallidurans* CH34, contains one metal-binding site per monomer. Both Ni and Co elicit a biological response and bind the protein in a 3N2O1S coordination sphere with a nearly identical octahedral geometry as shown by the X-ray structure of CnrXs, the soluble domain of CnrX. However, in solution CnrXs is titrated by 4 Co-equiv and exhibits an unexpected intense band at 384 nm that was detected neither by single-crystal spectroscopy nor under anaerobiosis. The data from a combination of spectroscopic techniques (spectrophotometry, electron paramagnetic resonance, X-ray absorption spectroscopy) showed that two sites correspond to those identified by crystallography. The two extra binding sites accommodate Co(II) in an octahedral geometry in the absence of oxygen and are occupied in air by a mixture of low-spin Co(II) as well as EPR-silent Co(III). These extra sites, located at the N-terminus of the protein, are believed to participate to the formation of peroxo-bridged dimers. Accordingly, we hypothesize that the intense band at 384 nm relies on the formation of a binuclear μ-peroxo Co(III) complex. These metal binding sites are not physiologically relevant since they are not detected in full-length NccX, the closest homologue of CnrX. X-ray absorption spectroscopy demonstrates that NccX stabilizes Co(II) in two-binding sites similar to those characterized by crystallography in its soluble counterpart. Nevertheless, the original spectroscopic properties of the extra Co-binding sites are of interest because they are susceptible to be detected in other Co-bound proteins.

The β-proteobacterium *Cupriavidus metallidurans* CH34 contains one of the most extensive collection of genetic determinants for metal resistance, making it the archetype of heavy-metal resistant bacteria.[1−4] Resistance mainly relies on its ability to encode redundant RND (resistance nodulation and cell division) heavy-metal efflux pumps. The setup of these detoxification complexes is generally controlled by two-component systems allowing the signal transduction from the periplasm to the cytoplasm. However, the expression of the CnrCBA efflux pump involved in cobalt and nickel resistance in *C. metallidurans* CH34 requires a three-protein transmembrane signal transduction complex called CnrYXH.[5−8] In this complex, CnrY and CnrX are membrane-anchored proteins. CnrX, which possesses a metal-sensor domain protruding in the

periplasm (CnrXs), interacts with the antisigma factor CnrY. The latter sequesters CnrH, an ECF-type (extracytoplasmic function) sigma factor, on the cytoplasmic side of the membrane. Metal resistance is induced by the specific release of CnrH from the CnrYX complex upon sensing of increasing amount of Ni or Co in the environment. CnrH is required for the RNA-polymerase to initiate transcription at *cnr* promoters.

We previously determined the three-dimensional structure of CnrXs, a soluble form of CnrX spanning residues 31−148, in different metal-bound forms (Cu, Ni, Co, Zn) as well as in an

apo-form represented by the E63Q-CnrXs mutant.[9−11] CnrXs is a dimer in which each protomer forms a four-helix bundle and contains one metal-binding site. Both Ni and Co ions elicit a biological response while Zn-bound CnrXs represents an inactive form of the complex. A dramatic change of the geometry of the metal-binding site is observed as a function of the bound metal ion: trigonal bipyramidal in the presence of Zn vs octahedral in the presence of Ni or Co. While the Zn ion is pentacoordinated in a 3N2O sphere, Ni or Co ions recruit the thioether sulfur of the only methionine (Met123) residue of the sequence as a sixth ligand. We have proposed that the recruitment of Met123 side chain is the qualitative change that switches on the sensing mechanism by remodeling the four-helix bundle around the metal-binding site.[11]

UV−vis spectra recorded during single-crystal spectroscopy analysis of Co-bound CnrXs exhibited the typical features of hexacoordinated high-spin Co(II). They are thus consistent with the X-ray structure of the metal-binding site. Morevover, these spectra are similar to those of Co-bound NccX, a membrane-bound full-length homologue of CnrX from *C. metallidurans* 31A.[3,11] This strongly suggests that CnrXs is a good structural model of the native protein. However, the Co titration of CnrXs in solution gave unforeseen and unprecedented spectra with an intense band at 384 nm saturating after the binding of 4 Co-equiv per dimer. This shows that CnrXs in solution contains extra-binding sites in addition to those determined by X-ray diffraction. Actually, we have previously demonstrated that the N-terminus sequence of CnrXs is probably involved in the formation of these extra-binding sites since the mutation of His32 for Ala produced a protein unable to display this intense band at 384 nm.[11] H32A-CnrXs is thus a good spectroscopic model of crystallized CnrXs.

As yet, it has not been possible to obtain NccX crystals or CnrXs crystals with more than two Co bound. However, the rich electronic properties of Co(II) make this metal ion a very useful spectroscopic probe. The spectrophotometric character-istics of 4 Co-bound CnrXs along with electron paramagnetic resonance (EPR) and X-ray absorption experiments (XAS) data led us to describe in this report the original spectroscopic properties of a novel Co-binding site that is susceptible to be detected in other Co-bound proteins. XAS was also used to further characterize the metal-binding sites of full-length NccX. The physiologic relevance of the different metal-binding sites is discussed.

■ EXPERIMENTAL PROCEDURES

Protein Preparation. CnrXs, E63Q-CnrXs, H32A-CnrXs, and NccX were overproduced and purified as previously described.[9−11] Protein concentrations were determined using the Bradford protein assay (BioRad) with bovine serum albumin as standard. Throughout this article, CnrXs refers to a dimer; therefore, all concentrations given are those of the dimeric protein.

Spectroscopic Methods. UV−vis spectra were recorded at room temperature in a quartz cell of 10 mm light path using a Cary 50 Bio (Varian) spectrophotometer. The cuvette was filled with 0.12 mL of CnrXs or CnrXs mutants at variable concentrations in 50 mM Hepes pH 8, 100 mM NaCl. A first spectrum corresponding to the *apo* form of the protein was recorded. Then, the desired amount of Co was added from a freshly prepared stock solution of CoCl$_2$ in water so that the

dilution was considered negligible. A spectrum was recorded immediately after each addition.

X-band EPR measurements were performed at 9.64 GHz with 100 kHz magnetic modulation and a microwave power of 2 mW on a Bruker EMX, equipped with the ER-4192 ST Bruker cavity and an ER-4131 VT. For cobalt, the EPR spectra were recorded at 12 K with an attenuation of 5 G, whereas for copper, the spectra were recorded at 35 K with an attenuation of 3 G. Each sample was constituted of CnrXs or mutants at a concentration of 400−500 μM in Hepes buffer, and the desired amount of CoCl$_2$ or CuCl$_2$ was added. Spectra were recorded as described in the corresponding legend. Simulations have been performed using the EasySpin program.[12] For the simulations of the $S = 3/2$ Co(II) EPR spectra, the spin Hamiltonian $H = \beta g S H + S D S$ has been used, with a positive D corresponding to an $M_s = |\pm^1/_2\rangle$ ground-state Kramers' doublet. Since for Co(II) $|D| \gg \beta g S H$,[13] an arbitrarily value of $D = 50$ cm^{-1} was assumed.

For XAS experiments, 100 μL of 1−2 mM sample was transferred right after preparation to a PEEK homemade five-cell sample holder with a Kapton window and flash-frozen in liquid nitrogen. X-ray absorption measurements were carried out at the European Synchrotron Radiation Facility (ESRF, Grenoble, France) which was operating with a ring current of 150−200 mA. Spectra were collected on the BM30B (FAME) beamline[14] using a Si(220) double crystal monochromator with dynamic sagital focusing. The photon flux was of the order of 10^{12} photons/s, and the spot size was 300 μm horizontal × 100 μm vertical (full width half-maximum values). The sample holder was loaded in a helium cryostat with temperature set to 10 K during data collection. All spectra were collected in fluorescence mode by measuring the Co Kα fluorescence with a 30-element solid-state Ge detector (Canberra). For each sample, four to six scans of 40 min each were averaged. Energy calibration was achieved by measuring a cobalt foil and assigning the first inflection point of the spectrum to 7709.0 eV. Data analysis was performed using the IFEFFIT package[15] including ATHENA for the data extraction and ARTEMIS for the shell fitting. E_0 was defined at the half-height of the absorption edge step. k^3-weighted EXAFS spectra were Fourier transformed over the k range 2.6−12.9 Å^{-1} using a Hanning window ($\alpha = 1.0$). Fits were performed on the Fourier filtered spectra over the R range 0.9−4.0 Å. Theoretical amplitude and phase shift functions were calculated with the *ab initio* code FEFF 6.0[16] using the structure of Co-bound CnrXs crystals determined by X-ray diffraction[11] and of *trans*-bis(imidazole)-bis(2-oximinopropionato-N,O)cobalt(III) monohydrate.[17] Var-ious Co(II) and Co(III) reference compounds were used for comparison with the protein spectra, including Co(II) acetate tetrahydrate, [Co(II)ac]; Co(II)(2-methylimidazole)$_4$(BF$_4$)$_2$, [Co(II)BF$_4$];[18] Co(III)BG2 (Cambridge Crystallographic Data Centre deposition number, CCDC 832088), Co(III) acetylacetonate, [Co(III)acac], and Co(III) ethylenediamine, [Co(III)en].

When anaerobiosis was required, the solutions were made oxygen-free by incubation in a glovebox under overpressure of nitrogen and nitrogen bubbling for the largest volumes. The mixture for spectrophotometric or EPR analyses were prepared in the glovebox. The spectrophotometric cuvettes or EPR tubes were hermetically closed with a rubber septum in order to keep them anaerobic before subsequent analysis.

Dimer Stabilization Analysis. CnrXs along with E63Q- and H32A-CnrXs were loaded with increasing amount of Co
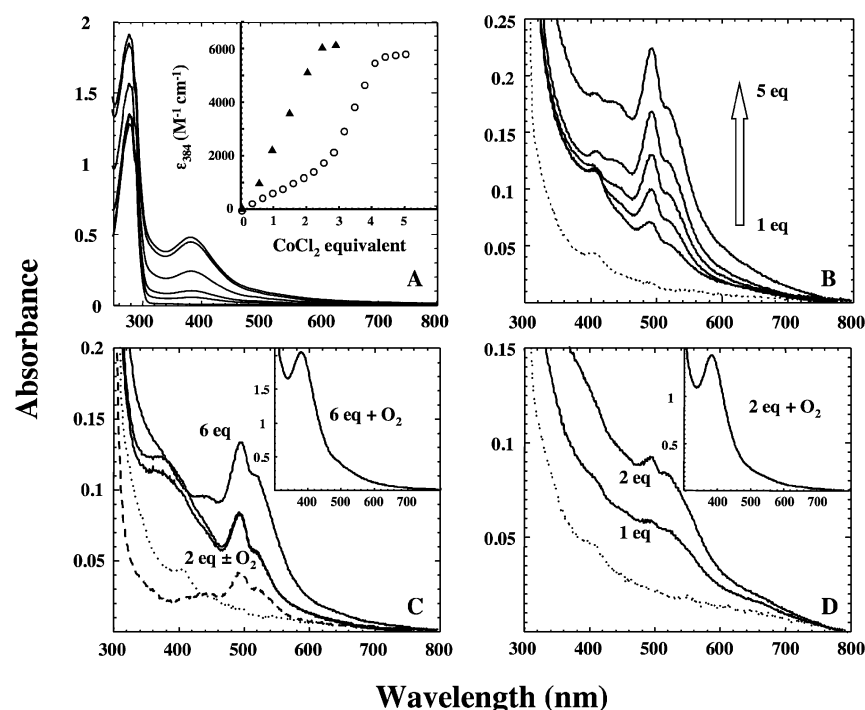
Figure 1. UV−vis spectroscopic characterization of CnrXs, E63Q-CnrXs, and H32A-CnrXs. All spectra were recorded in 50 mM Hepes (pH 8), 100 mM NaCl. (B−D) The spectra displayed in dotted line correspond to the *apo*-protein used in each experiment. (A) Aerobic titration of CnrXs (80 μM) with iterative addition of 1 equiv of CoCl$_2$. The inset shows the plot of the molar extinction coefficient at 384 nm of CnrXs (O) and E63Q-CnrXs (▲) as a function of the number of Co-equiv. (B) Anaerobic titration of CnrXs (564 μM) with iterative addition of 1 equiv of CoCl$_2$. (C) Absorption spectra of CnrXs (406 μM) after addition of 2 and 6 Co-equiv under anaerobiosis. The spectra were also recorded after opening to air (superimposition for 2 Co-equiv and insert for 6 Co-equiv). The spectrum of 2-Co-bound H32A-CnrXs (150 μM) is shown for comparison (dashed line). (D) Anaerobic titration of E63Q-CnrXs (511 μM) with iterative addition of 1 equiv of CoCl$_2$. The inset shows the spectrum of 2-Co-bound E63Q-CnrXs after opening to air.

ions, incubated overnight, and analyzed by SDS-PAGE without boiling the samples. In another experiment, CnrXs and E63Q-CnrXs were loaded with 4 Co-equiv and 2 Co-equiv, respectively, under anaerobiosis. Each sample was divided in two aliquots: one kept under inert atmosphere in the glovebox and the other opened to oxygen. After an overnight incubation, they were also analyzed by SDS-PAGE without boiling the samples.

■ RESULTS

Spectrophotometric Characterization of the Metal-Binding Sites in CnrXs. The X-ray structure of Co-bound CnrXs showed one binding site per monomer with a 3N2O1S coordination sphere for each metal ion.[11] A schematic representation of the Co-binding site, called site 1 in the following, is given in Figure SI1. It exhibited the typical features of a hexacoordinated high-spin Co(II),[19,20] as shown by the single-crystal visible spectrum of Co-bound CnrXs.[11] However, the titration of CnrXs in solution by stepwise addition of CoCl$_2$ gave different spectra (Figure 1A). The solution turned brownish, and the evolution of the UV−vis spectra was characterized by the concomitant increase of absorbance both at 280 and 384 nm, the reaction being complete at 4 equiv of Co. This increase was not linear. It displayed a first phase corresponding to the binding of 2 Co-equiv with an apparent average molar extinction coefficient of about 500 M^{-1} cm^{-1} per equivalent at 384 nm (ε_{384}), while the second phase corresponded to the binding of 2 extra Co-equiv with an average ε_{384} of 3000 M^{-1} cm^{-1} per equivalent at the same wavelength.

To further characterize the Co-binding properties of CnrXs, we have produced by site-directed mutagenesis the E63Q-CnrXs mutant in which glutamate was replaced by glutamine. Glu63 was demonstrated to be a bidentate ligand of Co(II) in the site 1.[11] As expected, the disappearance of two ligands dramatically affected the ability of the protein to accommodate Co ions in site 1. When E63Q-CnrXs was titrated by stepwise addition of CoCl$_2$, only two Co-binding sites per dimer were revealed with an average ε_{384} of about 3000 M^{-1} cm^{-1} per equivalent (Figure 1A, inset). This strongly suggests that CnrXs contains two extra metal-binding sites in addition to site 1 and explains why 4 Co-equiv was necessary to complete the CnrXs titration. As previously reported,[11] this second site, called site 2 in the following, could be eliminated by mutation of His32. The spectrum of Co-bound H32A-CnrXs is characterized by a major d−d transition band at 495 nm (ε around 75 M^{-1} cm^{-1}) with two shoulders at 435 and 525 nm (ref 11 and Figure 1C). Interestingly, this spectrum is essentially similar to that of CnrXs obtained under strict anaerobic conditions (Figure 1, panels B and C). Titration of CnrXs in the absence of oxygen led to a linear increase in absorbance at 435 nm, up to 4 Co-equiv (Figure 1B). Addition of a fifth Co-equiv caused a general increase of the spectrum assigned to adventitious binding. These results suggest that, in anaerobic conditions, both site 1 and site 2 bind high-spin Co(II) in a similar coordination geometry, demonstrated to be octahedral for site 1.[11] The influence of oxygen was further delineated by opening to air the spectroscopic cuvette after addition of either 2 Co-equiv or of an excess of cobalt (6 Co-equiv in Figure 1C). In the first case, the spectrum did not significantly change after oxygen addition.

In the second case on the contrary, the spectrum was immediately modified and corresponded to the one recorded in the presence of oxygen.

A similar experiment was performed with E63Q-CnrXs. Figure 1D shows the titration of this mutant by stepwise addition of 2 Co-equiv under anaerobiosis and the resulting spectrum after opening to air. The spectra of Co-bound E63Q-CnrXs recorded anaerobically resembled a smoothed version of Co-bound CnrXs or H32A-CnrXs, suggesting a mixture of species dominated by hexacoordinated high-spin Co(II). Opening to air after the addition of 2 Co-equiv led to a dramatic change, i.e., the appearance of an intense band centered at 384 nm. The hypothesis that this band was due to protein oxidation, linked to Co-binding to site 2 in the presence of oxygen, was ruled out because the molecular mass of the CnrXs was not affected, as checked by mass spectrometry (not shown). In addition, as CnrXs does not contain any cysteine, the band at 384 nm cannot be due to thiolate-S-to-Co ligand-to-metal charge transfer. Another hypothesis is that the large increase of absorbance at 384 nm could correspond to the evolution of the Co speciation in site 2.

EPR Spectroscopic Characterization of Co-Bound CnrXs. The titration of CnrXs by $CoCl_2$ was followed by EPR spectroscopy. The EPR spectra obtained after addition of 1, 2, or 4 Co(II)-equiv under anerobiosis, and the corresponding spectra recorded after opening the tubes to air are displayed on Figure 2 (upper panel). The spectra are consistent with high-spin $S = 3/2$ Co(II) centers. The integration of the low field part of the spectra can give an estimate of the evolution of the intensity of the high spin Co(II) signal and shows an almost linear increase in magnitude depending on the number of added Co-equiv. Exposure to air did not cause any visible change for both 1-Co(II)- and 2-Co(II)-bound CnrXs spectra, while the intensity of the 4-Co-bound CnrXs spectrum decreased 2-fold. This suggests that, in the presence of air, 2 equiv of Co(II) in the 4 Co-equiv sample have been transformed into EPR-silent species. It is noteworthy that an extra signal centered at $g = 2$ appeared concomitantly. It was assigned to a very small amount of low-spin Co(II). The appearance of this signal denotes a minor structural rearrangement around the metal ion. The EPR spectra obtained from the titration of E63Q-CnrXs by $CoCl_2$ still displayed a typical EPR signature that is typical of a high-spin Co(II) center, but the shape of the spectrum was completely different (Figure 2, middle panel). Opening to air led to the disappearance of this EPR signal and the concomitant appearance of the low-spin Co(II) signal. At the opposite, the EPR signature of two Co-bound H32A-CnrXs was similar to that of Co-bound CnrXs, and this signal remained insensitive to oxygen (Figure 2, lower panel).

The EPR analysis confirms that CnrXs contains four Co-coordination sites. Two Co(II) sites corresponding to site 1 are revealed in H32A-CnrXs, in which the Co(II) center remains insensitive to the presence of air. The other two coordination sites, present in E63Q-CnrXs, are assigned to site 2 in which Co(II) binds before to evolve into EPR-silent species which could be Co(III). The coordinating sites of several metalloproteins have been probed by EPR analysis of their high-spin Co(II)-substituted derivatives.[20−22] However, most of the reported spectra exhibit complicated line shapes. Their analysis is made difficult because $|D|$ is usually much greater than the Zeeman interaction (βgSH) for Co(II). It leads to X-band EPR spectra insensitive to the magnitude of D. Therefore, the only
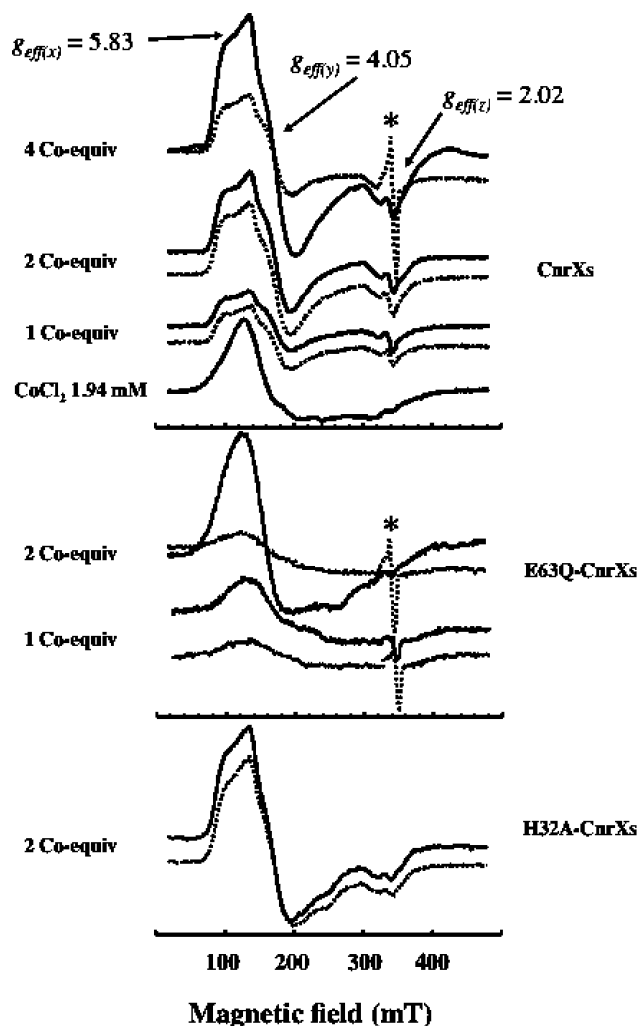

Figure 2. X-band EPR analysis of cobalt binding to CnrXs, E63Q-CnrXs, and H32A-CnrXs. Cobalt was added as $CoCl_2$ from a freshly prepared solution in water. EPR spectra corresponding to samples prepared under anaerobic conditions are shown in solid line. The resulting spectra recorded after opening the tubes to air are in dotted lines. The protein was used at a final concentration of 485 μM (CnrXs), 470 μM (E63Q-CnrXs), and 409 μM (H32A-CnrXs). As a control, the spectrum of free $CoCl_2$ at a concentration corresponding to 4 Co(II) equiv is shown in the upper panel. General EPR conditions are given in the Experimental Procedures section. The signal pointed by an asterisk (∗) was assigned to low-spin Co(II) ($S = 1/2$).

relevant EPR parameters that can be extracted are the g_{real} and E/D values.[23] Looking first at site 1, for which a typical EPR spectrum corresponds to two Co-bound CnrXs (simulation given in Figure SI2) or H32A-CnrXs in the presence of air, the turning points are located at $g_{eff(x,y,z)}$ = 2.02, 4.05, and 5.83. A plateau can be observed in the transition corresponding to about 510 G, in agreement with a hyperfine coupling of 73 G. This $A(^{59}Co)$ value is in the range (70−90 G) generally found in Co(II)-substituted proteins.[13,23] Therefore, the presence of an unresolved eight-line hyperfine pattern due to the $I = 7/2$ ^{59}Co can be suspected in the low-field absorption feature. Simulation of the experimental data provides the following spin-Hamiltonian parameters for the $M_s = |\pm^1/_2\rangle$: $g_{real(x,y)}$ = 2.45, $g_{real(z)}$ = 2.11, and E/D = 0.125. These parameters are close to those obtained with other Co(II)-containing proteins

and are indicative of either a five- or six-coordinate Co(II) center. Besides, the presence of [59]Co hyperfine splitting is consistent with a tetrahedral or octahedral geometry. Therefore, these results are in agreement with a six-coordinate environment for the Co(II) in site 1.[24] The E/D value also gives structural information, in particular the extent of deviation from idealized axial geometry. The E/D value of 0.125 is in agreement with a distorted geometry around the Co(II) center. In addition, the notable deviation of g_{real} from g_e shows a high degree of spin–orbit coupling, as would be expected for a high-spin Co(II) ion in a coordination environment with a relatively low symmetry. The EPR spectra obtained for E63Q-CnrXs recorded in anaerobic conditions corresponds to the signature of the Co(II) in site 2. It displays a large low-field absorbance with no resolvable rhombicity or [59]Co hyperfine structure. In addition, the highest field g feature is undetectable. In contrast to site 1, these parameters are consistent with a Co(II) center with much less constraint upon its geometry, characteristic of five- or six-coordinate Co(II) with at least one water ligand.

EPR Spectroscopic Characterization of Cu-Bound CnrXs. To go further in the characterization of CnrXs metal-binding sites, the titration of the protein by CuCl$_2$ has been followed by EPR spectroscopy (Figure 3). The EPR spectra are
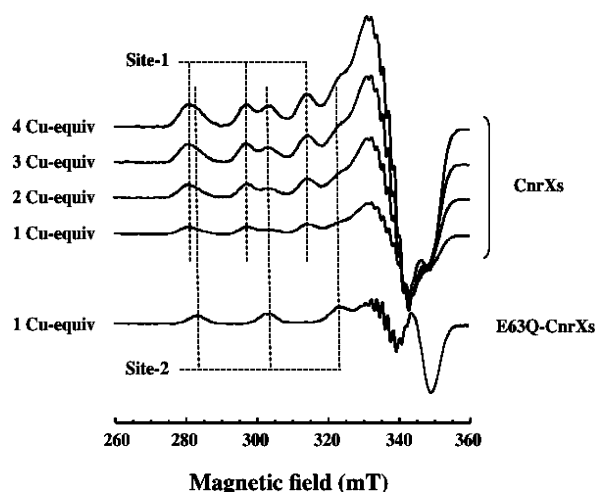
Figure 3. X-band EPR analysis of copper binding to CnrXs or E63Q-CnrXs. Copper was added as CuCl$_2$ from a freshly prepared solution in water. The protein was used at a final concentration of 485 μM (CnrXs) and 470 μM (E63Q-CnrXs). The specific features of site 1 or site 2 in the parallel region are depicted by dotted lines. General EPR conditions are given in the Experimental Procedures section.

consistent with $S = 1/2$ Cu(II) type 2 centers.[25] The complex pattern is indicative of a mixture of two types of Cu(II) sites contributing to all EPR spectra. The two sites can readily be distinguished by examination of the low field features corresponding to the [63]Cu hyperfine splitting ($I = 3/2$) in the $g_{\parallel}$ component. The EPR spectrum of the Cu(II)-bound E63Q-CnrXs (simulation given in Figure SI3), for which only site 2 is retained, was used to help the deconvolution of the Cu-bound CnrXs spectra. It reveals a unique $S = 1/2$ Cu(II) signature characterized by $g_{\parallel} = 2.194$ and $g_{\perp} = 2.028$ with [63]Cu hyperfine coupling of $A_{\parallel} = 625$ MHz. Superhyperfine interactions arising from $I = 1$ [14]N are also observed in the $g_{\perp}$ component with a very complicated pattern involving more than nine lines. Consequently, we can deduce that at least three nitrogen based ligands are involved in the coordination of the

Cu(II) in site 2. The subtraction of the signal corresponding to site 2 from the 4 Cu-equiv CnrXs signal leads to the EPR signature of site 1 (simulation given in Figure SI4) characterized by an axial signal $g_{\parallel} = 2.267$ and $g_{\perp} = 2.054$ with a [63]Cu hyperfine coupling of $A_{\parallel} = 525$ MHz. These parameters are similar to those previously reported, assigned to the site 1 of CnrXs, in which the Cu(II) ion was coordinated to three histidines and one glutamate in the equatorial plane.[9] The ratio of the intensity of the features observed at 297 and 303 mT, arising from the two different coordination sites during the titration of CnrXs by CuCl$_2$, varies from 60/40 to 50/50 (site 1/site 2) when the number of equivalents of added Cu(II) increases from 1 to 4.

Competition between Cu(II)- and Co(II)-Binding Investigated by EPR. The relative affinity of the two different coordination sites of CnrXs for Co(II) and Cu(II) has been tested. Two series of experiments were performed, in which 2 equiv of one metal ion was added to CnrXs, prior to the addition of 2 equiv of the other metal ion in the presence of air. The resulting EPR spectra are depicted in Figure 4. The
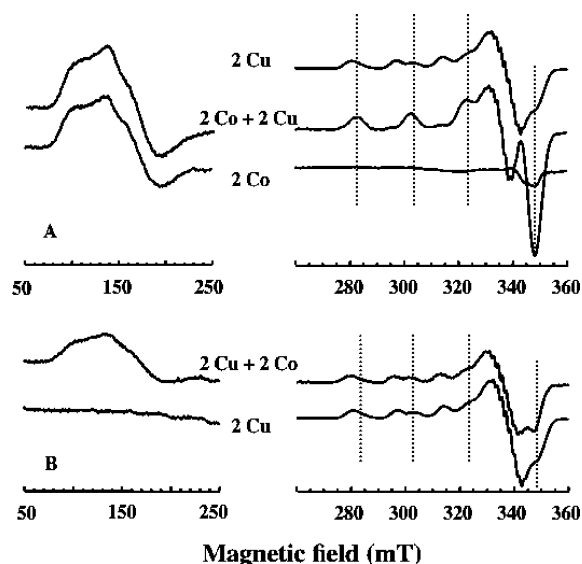
Figure 4. EPR analysis of the competition for Cu(II)- and Co(II)-binding to CnrXs. CnrXs (225 μM) was first loaded by 2 Co-equiv (panel A) or 2 Cu-equiv (panel B). Then, after recording the first EPR spectrum, 2 equiv of the second metal ion was added. The protein was used at a final concentration of 255 μM. The specific features of Cu(II) bound to site 2 is indicated by the vertical dotted lines. For clarity, the low-field resonance (50−250 mT) was magnified, and the spectrum of 2-Cu-bound CnrXs was added in panel A.

addition of 2 Cu(II)-equiv on 2 Co-bound CnrXs led to a unique Cu(II) signal corresponding to that of site 2, without change in the Co(II) EPR spectrum (Figure 4, panel A). This unambiguously shows that the first 2 equiv of Co(II) preferentially bind to site 1 and are not displaced by the successive addition of Cu(II), demonstrating a higher affinity of Co(II) as compared to Cu(II) for site 1. Conversely, the addition of 2 Co(II)-equiv on the 2 Cu-bound CnrXs led to the appearance of a high-spin Co(II) EPR spectrum, corresponding to a small amount of Co(II) bound to site 1. The rest of the added Co(II) was probably converted into an EPR-silent species when bound to site 2 in the presence of air. It should be noted that Co(III) directly added to the protein solution could not bind CnrXs (not shown). Furthermore, small changes can

be observed between the Cu(II) EPR spectra. The ratio of the intensity of the two different sites slightly varies for the benefit of site 2. This result suggests that the affinity of Cu(II) for the two sites is comparable but that Co(II) is capable to partly displace Cu(II) from site 1.

Metal Site Structures Explored by X-ray Absorption Spectroscopy. NccX is the homologue of membrane-bound full-length CnrX, for which purification has been so far unsuccessful. We have already described the purification and the preliminary spectrophotometric characterization of full-length NccX.[11] NccX binds only 2 Co-equiv, with the spectroscopic signature of site 1, suggesting that site 2 is absent in the full-length form of the protein. Owing to difficulty of crystallization, NccX is not known in atomic details. XAS was thus used to further characterize the Co-binding sites in NccX. XAS was also used to explore the site 1 and site 2 structures of CnrXs in solution. Figure 5 shows the XANES spectra for 2 Co-
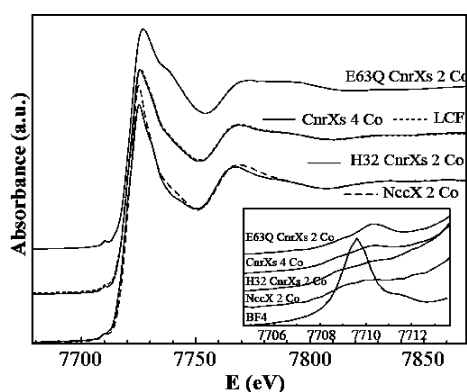

Figure 5. Co K-edge XANES spectra for 2-Co-bound E63Q-CnrXs, 4-Co-bound CnrXs, 2-Co-bound H32A-CnrXs, and NccX. The dotted line superimposed on 4-Co-bound CnrXs is a linear combination fit obtained with 62% 2-Co-bound H32A-CnrXs + 36% 2-Co-bound E63Q-CnrXs. Inset: close-up view the pre-edge feature and comparison with Co(2-methylimidazole)$_4$(BF$_4$)$_2$.

bound E63Q-CnrXs, 4 Co-bound CnrXs, 2 Co-bound H32A-CnrXs, and 2 Co-bound NccX. Co XANES spectra generally present a pre-edge peak at about 7710 eV assigned to a mixture of quadrupole 1s–3d and dipole 1s–4p transitions, whose intensity decreases when the degree of symmetry of the polyhedron or the degree of occupancy of the 3d shell increases.[26–28] The pre-edge is more intense for Co tetrahedral (such as Co(II)BF4 in Figure 5) than for octahedral coordination and for Co(III) than for Co(II) (Figure SI5). All the spectra shown in Figure 5 present a weak pre-edge peak between 7709 and 7711 eV as compared to Co(II)BF$_4$. This comparison suggests an octahedral coordination for Co in all the protein samples. The spectra for 2-Co-bound H32A-CnrXs and 2-Co-bound NccX show an edge at the same position as that of Co(II) acetate tetrahydrate (Figure SI5). This observation is consistent with the presence of divalent Co in these samples.

The EXAFS spectra for 2 Co bound H32A-CnrXs and 2 Co-bound NccX and their shell fits are shown in Figure 6. The derived structural parameters are given in Table 1. In 2-Co-bound H32A-CnrXs, the metal is bound to 3 His at 2.11 Å, 2 O atoms at 2.13 Å, and 1 S atom at 2.57 Å. Multiple scattering contributions within the imidazole ring are responsible for the peaks situated between $R + \Delta R$ = 2.5 and 4.0 Å (Figure 6B).

These parameters are in good agreement with the structure of site 1 of CnrXs determined by the X-ray diffraction,[11] with Co–N (from His) interactions at 2.11, 2.11, and 2.12 Å, Co–O (Glu63) interactions at 2.13 and 2.16 Å, and Co–S (Met123) interactions at 2.54 Å. The spectrum for 2-Co-bound NccX presents strong similarities with that of 2-Co-bound H32A-CnrXs. Accordingly, its structural parameters are very close to those detailed above, with 3 His, 2 O, and 1 S atomic neighbors (Table 1).

On the contrary, 2-Co-bound E63Q-CnrXs exhibits strongly different XANES and EXAFS spectra and Fourier transforms (Figures 5 and 6). The position of the absorption edge for 2-Co-bound E63Q-CnrXs is shifted to higher energy relative to 2-Co-bound H32A-CnrXs and NccX. The XANES part was fitted by a combination of 59% 2-Co-bound H32A-CnrXs (or 2-Co-bound NccX) + 39% [Co(III)acac] (Figure SI5). This suggests the presence of both divalent and trivalent Co in this sample. The EXAFS spectrum for 2-Co-bound E63Q-CnrXs has a markedly lower frequency and amplitude than 2-Co-bound H32-CnrXs and NccX. No good fit was obtained supposing divalent Co only (with ΔE values = 9 ± 1 eV, as found for the model compounds) or trivalent Co only (ΔE values = 2 ± 1 eV, as found for the model compounds). A satisfactory fit was obtained with 2 His bound to Co(II), plus 2.0 N/O ligands and 0.5 His bound to Co(III) (Table 1 and Figure 6). Interestingly, the contributions of the first shells of Co(II) and Co(III) are in complete opposition of phase (Figure SI6), resulting in a destructive interference (cancellation of the signal of the two contributions). In the present case, the resulting FT peak is both relatively narrow and situated at shorter distance relative to the two individual contributions. Provided that all Co atoms in 2-Co-bound E63Q-CnrXs are present in site 2, these results suggest that site 2 is occupied by both Co(II) and Co(III) and that some His ligands are involved. Keeping in mind that the EXAFS signal provides information on the average local environment over the different Co sites in the samples, the average number of ligands for Co determined by EXAFS fit equals 4.5. Theoretically, these results may correspond to 40% of Co(II) bound to 5 ligands (N = 2.0) and 60% of Co(III) bound to 4 ligands (N = 2.4) or 50% of Co(II) bound to 4 ligands (N = 2.0) and 50% of Co(III) bound to 5 ligands (N = 2.5). Because of the destructive interference between the contributions of Co(II) and Co(III), the number of ligands is probably underestimated. We know from the X-ray structure of Co-bound CnrXs and from the XAS analysis of 2-Co-bound H32A-CnrXs that site 1 is octahedral. The number of ligands being similar for Co(II) and Co(III) (2.0 and 2.5), it is likely that site 2 is octahedral as well.

The XANES and EXAFS spectra for 4-Co-bound CnrXs are intermediate between 2-Co-bound H32A-CnrXs (or NccX) and 2-Co-bound E63Q-CnrXs. The first peak for 4-Co-bound CnrXs is double, with a maximum at 1.65 Å and a shoulder at 1.35 Å. Both the XANES and the EXAFS parts were correctly fitted by a linear combination of about 60% 2-Co-bound H32A-CnrXs and about 40% 2-Co-bound E63Q-CnrXs (Figures 5 and 6). Imposing a 50–50 distribution clearly altered the fit quality. Thus, Co environments and valence states found in 4 Co-bound CnrXs are slightly different from the simple addition of those found in 2-Co-bound H32A-CnrXs and 2-Co-bound E63Q-CnrXs.

Site 2 Is Involved in Stabilization of the CnrXs Dimer. Figure 7A indicates that in the absence of added cobalt CnrXs and the mutant proteins were denatured to monomer while
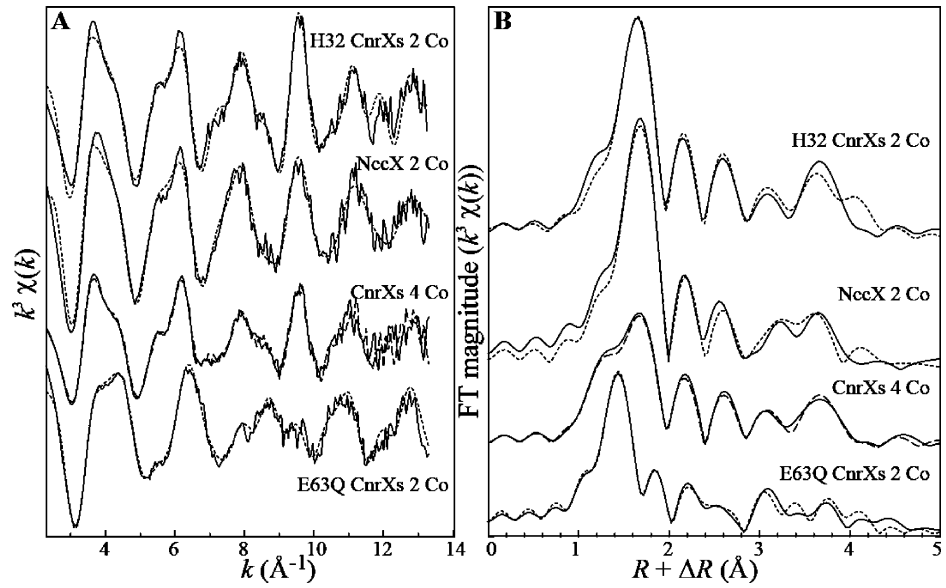
Figure 6. Co K-edge EXAFS spectra (A) and Fourier transforms moduli (B) for 2-Co-bound E63Q-CnrXs, 4-Co-bound CnrXs, 2-Co-bound H32A-CnrXs, and 2-Co-bound NccX. The dotted lines superimposed on 2-Co-bound E63Q-CnrXs, 2-Co-bound H32A-CnrXs, and 2-Co-bound NccX are multishell fits, and the dashed line superimposed on 4-Co-bound CnrXs is a linear combination fit obtained with 56% 2-Co-bound H32A-CnrXs + 32% 2-Co-bound E63Q-CnrXs.

Table 1. Structural Environment for Co in 2-Co-Bound Forms of H32A-CnrXs, NccX and E63Q-CnrXs Obtained from EXAFS Data Analysis[a]

	atom	N	R (Å)	σ^2 (Å^2)	ΔE (eV)[b]	R factor
H32-CnrXs 2 Co	His[c]	3.0 ± 0.2	2.11 ± 0.04	0.004	8.0	1.6 × 10^{-2}
	O	2.0 ± 0.2	2.13 ± 0.07	0.009	8.0	
	S	0.9 ± 0.1	2.57 ± 0.02	0.005	8.0	
NccX 2 Co	His[c]	3.0 ± 0.2	2.09 ± 0.02	0.005	8.2	2.1 × 10^{-2}
	O	2.0 ± 0.2	2.13 ± 0.04	0.003	8.2	
	S	1.1 ± 0.1	2.57 ± 0.02	0.010	8.2	
E63Q-CnrXs 2 Co	His[c] (Co(III))[d]	0.5 ± 0.2	1.93 ± 0.003	0.003	2.0	5.0 × 10^{-3}
	N/O (Co(III))[d]	2.0 ± 0.2	1.93 ± 0.003	0.003	2.0	
	His[c] (Co(II))	2.0 ± 0.1	2.13 ± 0.005	0.003	10.0	

[a]N: number of atoms, R: interatomic distance, s^2: Debye−Waller factor, ΔE (eV): difference between the theoretical and experimentally determined threshold energies; R factor: residual between fit and experiment.. [b]Values of 9 ± 1 eV correspond to Co(II), and values of 2 ± 1 eV correspond to Co(III). [c]Including multiple scattering within the imidazole ring. [d]A single Co(III)−N was used for the fit, which was then separated between Co(III)−His (N = 0.5 based on the multiple scattering contributions) and Co(III)−N/O.
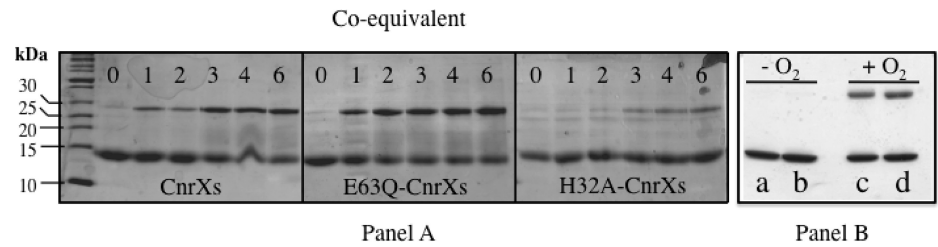

Figure 7. SDS-PAGE analysis of the cobalt titration of CnrXs, E63Q-CnrXs, and H32A-CnrXs. Panel A: protein was loaded with the indicated amount of CoCl$_2$, incubated overnight at 4 °C and loaded on 15% acrylamide SDS-PAGE without boiling. Panel B: 4-Co-bound CnrXs or 2-Co-bound E63Q-CnrXs were prepared anaerobically and then analyzed after overnight incubation in the presence or the absence of oxygen, as indicated. Lanes a and c: 4-Co-bound CnrXs. Lanes b and d: 2-Co-bound E63Q-CnrXs.

some of the dimeric form was retained in the presence of cobalt. Small amounts of dimeric CnrXs are resistant to denaturation in the presence of 1 or 2 Co-equiv. The proportion of CnrXs dimers detected reached a plateau from 3 Co-equiv and higher. The highest ratio of dimeric E63Q-CnrXs was readily obtained with 2 Co-equiv, and this ratio did

not increase for higher amount of cobalt. Conversely, the dimeric form of H32A-CnrXs was virtually invisible at 1 and 2 Co-equiv, and only a very small amount of dimer was detected for 3 Co-equiv and beyond. As shown in Figure 7B, the presence of oxygen is required for the stabilization of the dimer, and this effect depends on the presence of Co ions in site 2. It

is noteworthy that Cu(II), Zn(II), and Ni(II) did not contribute to stabilize the dimeric form of CnrXs (not shown).

■ DISCUSSION

CnrX is a 148 amino acid protein with 26 N-terminal residues serving as a membrane anchor. A soluble form of CnrX spanning residues 31 to 148 was produced, which we referred to as CnrXs.[9,10] This truncated protein was characterized as the metal-sensor domain of CnrX.[11] Crystallization of dimeric Co-bound CnrXs revealed one Co-binding site per monomer, called site 1 in this paper. The coordination sphere consisted of the Nε2 atoms of His42, -46, and -119 and one O of Glu63 side chain in the equatorial plane. The octahedral coordination sphere was completed with two axial ligands: the second oxygen of Glu63 carboxylate and the thioether sulfur of Met123 (Figure SI1). Accordingly, single-crystal spectroscopy gave the UV−vis spectrum expected for a slightly distorted six-coordinate high-spin Co(II). However, when CnrXs was titrated by $CoCl_2$ in the presence of oxygen, the protein solution turned brownish, and the resulting UV−vis spectra were dominated by an intense band centered at 384 nm that increased in two steps upon addition of Co. These two steps were characterized by different extinction coefficients up to the addition of 4 Co-equiv. This suggests that CnrXs dimer contained, in addition to site 1, two extra and original metal-binding sites, referred to as site 2. Preliminary affinity measurements were performed by isothermal titration calorimetry (ITC). In agreement with spectrocopic data, ITC experiments (Supporting Information, Table SI1) detected two types of Co-binding sites with affinities in the 1−100 nM range. The affinity of Co for both site 1 and site 2 was greatly affected upon mutation of Glu63 and His32, respectively. These preliminary data must be considered as qualitative. Accurate quantitative assessment of the thermodynamics parameters related to Co-binding requires further work. Actually, the calculated decrease of about 3 orders of magnitude is probably overestimated since it is not consistent with the spectroscopic data showing that these mutations caused the loss of metal binding to the mutated sites. The overestimation of the affinity values may reflect the complexity of the metal binding event to the protein.[29] This is particularly true for the thermodynamics of the Co-binding event to site 2 that is highly complex since it includes binding of Co(II), partial oxidation to Co(III), and probably slight conformational modifications as judged from the appearance of low-spin Co(II) detected by EPR.

The two identified Co-binding sites of CnrXs were further characterized with two major goals: (i) the characterization of the metal-binding sites in proteins reluctant to crystallization, i.e. full-length CnrX or its homologue NccX, and (ii) the biophysical characterization of site 2 that exhibits an unexpected UV−vis spectrum upon Co-binding. Inspection of the CnrXs sequence to identify putative extra Co ligands revealed three histidine residues in addition to those present in site 1. Among these residues, involvement of His131 in the coordination sphere of site 2 was unlikely because its mutation did not cause any effect on the UV−vis titration of CnrXs by Co ions (not shown). The two others (His32 and His38) belong to the nine amino acids sequence at the N-terminus of CnrXs, 31-SHRNEAGHG-39. With two histidine residues and a glutamate, this sequence that is not structurally defined could potentially participate to the formation of a metal-binding site in solution. Indeed, the mutation of His32 for Ala hampered

the formation of site 2.[11] E63Q-CnrXs that essentially binds 2 Co-equiv in site 2 is perfectly suited to characterize this metal-binding site. Under anaerobic conditions, Co(II) is stabilized in the high-spin state and appears to be either five-coordinate or six-coordinate with at least one water ligand in the site with few constraints as judged from the broad UV−vis spectrum and the lack of rhombicity and hyperfine structure in the low-field resonance of the EPR spectrum. EPR spectroscopy revealed that Co(II) was immediately changed to an EPR-silent species upon addition of air, although a small proportion remained as low-spin Co(II). XANES data were in agreement with Co in octahedral coordination and suggested that site 2 was occupied by a mixture of Co(II) and Co(III). The analysis of the EXAFS part confirmed these findings and showed the presence of His ligands in site 2. However, owing to the destructive interference of Co(II) and Co(III) contributions, it was difficult to conclude on the proportion of each species as well as on the exact coordination number for Co in site 2. Provided that the Cu coordination sphere resembles that of Co in site 2, as it is the case for site 1,[9,11] copper was used as a probe to better characterize site 2 by EPR. One Cu-bound E63Q-CnrXs exhibits an axial EPR signal whose parameters, low $g_\parallel$ value associated with large $A_\parallel$ value, can be consistent with a N4 coordination sphere in the equatorial plane according to the Peisach−Blumberg correlations.[25] At least three nitrogen-based ligands were estimated from the complex superhyperfine pattern observed in the high-field resonance. The detection of CnrXs dimers under soft electrophoretic conditions in the samples with site 2 intact suggests that coordination of the metal ion involves residues from the two monomers.

As shown by UV−vis spectroscopy, site 2 does not exist in full-length NccX or in Co-bound CnrXs crystals.[11] This raises the question of the relevance of such a site. Actually, a physiological role was ruled out by an *in vivo* study.[8] In *C. metallidurans* CH34 carrying the H32R single or the H32R/H38R double mutation in CnrX, nickel was still an inducer of resistance. Moreover, the H32R/H38R double mutation did not prevent CnrX to bind nickel. It was thus concluded that alteration of these residues did not abolish nickel-dependent induction of the *cnr* determinant and are probably not involved in Ni-binding[8] *in vivo*. Because CnrXs is a truncated form of the full-length protein, the degree of freedom of the N-terminal end is assumed to be higher and an adventitious Co-binding site can be formed *in vitro*. H42R/H46R double mutation diminished Ni-binding and almost completely abolished inducibility as well as metal resistance, making His42 and His46 of central importance for regulation by CnrX.[8] These ligands belong to the coordination sphere of Co in site 1.[9,11] UV−vis spectroscopic characterization of H32A-CnrXs, 2-Co-bound CnrXs under anaerobiosis, and 2-Co-bound NccX gave similar spectra (Figure 1C), suggesting a similar coordination sphere. XAS characterization of Co-bound NccX confirmed that the full-length protein can accommodate Co(II) in a metal-binding site comparable to that of H32A-CnrXs, in terms of ligand identity and of metal-to-ligand distances. As NccX is not able to bind more than 2 Co-equiv specifically, site 1 is probably the only metal-binding site present in the full-length protein. H32A-CnrXs is the best spectroscopic model of NccX, and probably of CnrX, since the close sequence similarity between these proteins (75% identity) includes a strict conservation of the His residues.

It is noteworthy that upon addition of 2 Co-equiv in the absence of oxygen, only site 1 is filled and the Co ions are

stabilized as Co(II). When the same experiment is performed in air, a part of Co ions are accepted by site 2 and appeared immediately oxidized to Co(III), causing the appearance of a band at 384 nm with an apparent molar extinction coefficient of 500 M^{-1} cm^{-1}. This apparent molar extinction coefficient is high enough to mask the absorption due to the binding of Co(II) to site 1 that is characterized by an absorbance centered at 495 nm and an ε_{495} around 75 M^{-1} cm^{-1}. Once site 1 is filled, cobalt binds exclusively to site 2 that exhibits a strong absorbance band at 384 nm characterized by an ε_{384} of 3000 M^{-1} cm^{-1}. This explains the biphasic titration of CnrXs by $CoCl_2$ in the presence of oxygen. It is known that octahedral Co(II) polyamine chelates, such as aqueous ammonia solutions containing Co(II) salts, turn brown on exposure to oxygen and that a diamagnetic salt of binuclear μ-peroxo cobalt(III) complex, $[(NH_3)_5CoO_2Co(NH_3)_5]^{4+}$, can be subsequently isolated and crystallized.[30−32] The bridging O−O ligand originates entirely from gaseous oxygen and contributes to form μ-peroxo dimers. The factors governing the ability of a Co(II) complex to pick up O_2 are not fully understood. However, it is well admitted that a water ligand can be easily displaced by O_2, and it has been hypothesized that such a complex must contain three donor nitrogen atoms as a minimum requirement for O_2 uptake.[33] Moreover, these six-coordinate μ-peroxo Co(III) complexes display strong charge-transfer bands around 350 nm with ε in the range 10^3–10^4 M^{-1} cm^{-1}.[34] Finally, slow transformation of these binuclear complexes to mononuclear Co(III) complexes has been also evidenced.[31] The local structure of Co in site 2 as determined in this study (5- or 6-fold coordination, with N-containing ligands and one water molecule) suggests that such a binuclear μ-peroxo Co(III) complex may be formed in Co-bound CnrXs. This hypothesis would be consistent with most of our results: (i) strong charge-transfer bands at 384 nm observed by spectrophotometry in the presence of oxygen, (ii) decrease of the intensity of the EPR spectra upon introduction of air due to the formation of diamagnetic dinuclear Co complexes, and to Co(II) oxidation to Co(III), and (iii) oxygen-dependent stabilization of CnrXs dimers observed by SDS-PAGE through a bridging dinuclear complex involving site 2. The presence of peroxo Co dimers would generate a Co—Co contribution at 4.3−4.5 Å,[30] depending on the geometry of the Co−O−O−Co chain in the EXAFS signal. Adding such a contribution to the EXAFS fit of 2-Co-bound E63Q-CnrXs (1 Co neighbor per Co(III) atom) did not affect the fit quality. Consequently, the formation of peroxo-bridged dimers is compatible with our EXAFS data. The high proportion of Co(II) observed by XAS remains puzzling but could be due to transient species in a slow oxidation process.[33,35]

C. metallidurans CH34 prevails in heavy-metal-rich environments,[1] and the metal-binding sites of the sensor-protein CnrX can be occupied by unspecific metal ions such as copper or zinc depending on natural or anthropogenic conditions. We already demonstrated that Ni and Co have a comparable affinity for CnrXs, both higher than that of Zn.[11] Now we have used EPR to compare the relative affinity of Co and Cu for site 1. We concluded that Cu(II) added after the first 2 equiv of Co(II) filled site 2 without displacing Co from site 1. Conversely, Co is able to partly displace Cu that is already present in site 1. This demonstrates that, upon increasing environmental concentration of Ni or Co ions, the Cnr system can easily be turned on by substituting Zn or Cu, two of the most abundant environmental metal elements, at the CnrXs metal-binding site.

■ AUTHOR INFORMATION

Corresponding Author
*Tel: 33-(0)4-38-78-24-03. Fax: 33-(0)4-38-78-54-94. E-mail: jacques.coves@ibs.fr.

■ ABBREVIATIONS

Cnr, cobalt and nickel resistance; EPR, electronic paramagnetic resonance; EXAFS, extended X-ray absorption fine spectroscopy; XANES, X-ray absorption near-edge structure; XAS, X-ray absorption spectroscopy.

■ REFERENCES

(1) Mergeay, M., Nies, D., Schlegel, H. G., Gerits, J., Charles, P., and Van Gijsegem, F. (1985) *Alcaligenes eutrophus* CH34 is a facultative chemolithotroph with plasmid-bound resistance to heavy metals. *J. Bacteriol. 162*, 328−334.

(2) Monchy, S., Benotmane, M. A., Janssen, P., Vallaeys, T., Taghavi, S., van der Lelie, D., and Mergeay, M. (2007) Plasmids pMOL28 and pMOL30 of *Cupriavidus metallidurans* are specialized in the maximal viable response to heavy metals. *J. Bacteriol. 189*, 7417−7425.

(3) von Rozycki, T., and Nies, D. H. (2009) *Cupriavidus metallidurans*: evolution of a metal-resistant bacterium. *Antonie Van Leeuwenhoek 96*, 115−39.

(4) Janssen, P. J., Van Houdt, R., Moors, H., Monsieurs, P., Morin, N., Michaux, A., Benotmane, M. A., Leys, N., Vallaeys, T., Lapidus, A., Monchy, S., Médigue, C., Taghavi, S., McCorkle, S., Dunn, J., van der Lelie, D., and Mergeay, M. (2010) The complete genome sequence of *Cupriavidus metallidurans* strain CH34, a master survivalist in harsh and anthropogenic environments. *PLoS One 5*, e10433.

(5) Liesegang, H., Lemke, K., Siddiqui, R. A., and Schlegel, H. G. (1993) Characterization of the inducible nickel and cobalt resistance determinant *cnr* from pMOL28 of *Alcaligenes eutrophus* CH34. *J. Bacteriol. 175*, 767−778.

(6) Grass, G., Grosse, C., and Nies, D. H. (2000) Regulation of the *cnr* cobalt and nickel resistance determinant from *Ralstonia* sp. strain CH34. *J. Bacteriol. 182*, 1390−1398.

(7) Tibazarwa, C., Wuertz, S., Mergeay, M., Wyns, L., and van Der Lelie, D. (2000) Regulation of the *cnr* cobalt and nickel resistance determinant of *Ralstonia eutropha* (*Alcaligenes eutrophus*) CH34. *J. Bacteriol.* 182, 1399–1409.

(8) Grass, G., Fricke, B., and Nies, D. H. (2005) Control of expression of a periplasmic nickel efflux pump by periplasmic nickel concentrations. *Biometals* 18, 437–448.

(9) Pompidor, G., Maillard, A. P., Girard, E., Gambarelli, S., Kahn, R., and Covès, J. (2008) X-ray structure of the metal-sensor CnrX in both the apo- and copper-bound forms. *FEBS Lett.* 582, 3954–3958.

(10) Pompidor, G., Girard, E., Maillard, A., Ramella-Pairin, S., Kahn, R., and Covès, J. (2009) Biostructural analysis of the metal-sensor domain of CnrX from *Cupriavidus metallidurans* CH34. *Antonie van Leeuwenhoek* 96, 141–148.

(11) Trepreau, J., Girard, E., Maillard, A. P., de Rosny, E., Petit-Haertlein, I., Kahn, R., and Covès, J. (2011) Structural basis for metal sensing by CnrX. *J. Mol. Biol.* 408, 766–779.

(12) Stoll, S., and Schweiger, A. J. (2006) EasySpin, a comprehensive software package for spectral simulation and analysis in EPR. *J. Magn. Reson.* 178, 42–55.

(13) Bennett, B., and Holz, R. C. (1997) EPR studies of the mono- and dicobalt(II)-substituted froms of the aminopeptidase from *Aeromonas proteolytica*. Insight into the catalytic mechanism of dinuclear hydrolases. *J. Am. Chem. Soc.* 119, 1923–1933.

(14) Proux, O., Nassif, V., Prat, A., Ulrich, O., Lahera, E., Biquard, X., Menthonnex, J.-J., and Hazemann, J.-L. (2006) Feedback system of a liquid-nitrogen-cooled double-crystal monochromator: design and performances. *J. Synchrotron Radiat.* 13, 59–68.

(15) Ravel, B., and Newville, M. (2005) ATHENA and ARTEMIS: Interactive graphical data analysis using IFEFFIT. *J. Synchrotron Radiat.* 12, 537–541.

(16) Rehr, J. J., Mustre de Leon, J., Zabinsky, S. I., and Albers, R. C. (1991) Theoretical X-ray absorption fine structure standards. *J. Am. Chem. Soc.* 113, 5135–5145.

(17) Lampeka, R. D., Uzakbergenova, Z. D., and Skopenko, V. V. (1993) Spectroscopic and X-ray investigation of cobalt(III) complexes with 2-oximinocarboxylic acids. *Z. Naturforsch.* 48b, 409–417.

(18) Adrait, A., Jacquamet, L., Le Pape, L., Gonzalez de Peredo, A., Aberdam, D., Hazemann, J.-L., Latour, J.-M., and Michaud-Soret, I. (1999) Spectroscopic and saturation magnetization properties of the manganese- and cobalt-substituted Fur (ferric uptake regulation) protein from *Escherichia coli*. *Biochemistry* 38, 6248–6260.

(19) Bertini, I., and Luchinat, C. (1984) High spin cobalt(II) as a probe for the investigation of metalloproteins. *Adv. Inorg. Biochem.* 6, 71–111.

(20) Maret, W., and Vallee, B. L. (1993) Cobalt as probe and label of proteins. *Methods Enzymol.* 226, 52–71.

(21) Fielding, A. J., Kovaleva, E. G., Farquhar, E. R., Lipscomb, J. D., and Que, L. Jr (2011) A hyperactive cobalt-substituted extradiol-cleaving catechol dioxygenase. *J. Biol. Inorg. Chem.* 16, 341–355.

(22) Breece, R. M., Costello, A., Bennett, B., Sigdel, T. K., Matthews, M. L., Tierney, D. L., and Crowder, M. W. (2005) A five-coordinate metal center in Co(II)-substituted VanX. *J. Biol. Chem.* 280, 11074–11081.

(23) Bennett, B. (2002) EPR of Co(II) as a structural and mechanistic probe of metalloprotein active sites: characterisation of an aminopeptidase. *Curr. Top. Biophys.* 26, 49–57.

(24) Werth, M. T., Tang, S. F., Formicka, G., Zeppezauer, M., and Johnson, M. K. (1995) Magnetic circular dichroism and electron paramagnetic resonance studies of cobalt-substituted horse liver alcohol dehydrogenase. *Inorg. Chem.* 34, 218.

(25) Peisach, J., and Blumberg, W. E. (1974) Structural implications derived from the analysis of electron paramagnetic resonance-spectra of natural and artificial copper proteins. *Arch. Biochem. Biophys.* 165, 691–708.

(26) Moen, A., Nicholson, D. G., Ronning, M., Lamble, G. M., Lee, J. F., and Emerich, H. (1997) X-Ray absorption spectroscopic study at the cobalt K-edge on the calcination and reduction of the microporous

cobalt silicoaluminophosphate catalyst CoSAPO-34. *J. Chem. Soc., Faraday Trans.* 93, 4071–4077.

(27) Jacobs, G., Patterson, P. M., Zhang, Y., Das, T., Li, J., and Davis, B. H. (2002) Fischer–Tropsch synthesis: deactivation of noble metal-promoted Co/Al$_2$O$_3$ catalysts. *Appl. Catal., A* 233, 215–226.

(28) Juhin, A., de Groot, F., Vanko, G., Calandra, M., and Brouder, C. (2010) Angular dependence of core hole screening in LiCoO2: A DFT+U calculation of the oxygen and cobalt K-edge x-ray absorption spectra. *Phys. Rev. B* 81, 115115.

(29) Wilcox, D. E. (2008) Isothermal titration calorimetry of metal ions binding to proteins: an overview of recent studies. *Inorg. Chim. Acta* 361, 857–867.

(30) Schaeffer, W. P. (1968) Structure of decaammine-μ-peroxo-dicobalt disulfate tetrahydrate. *Inorg. Chem.* 7, 725–731.

(31) Simplicio, J., and Wilkins, R. G. (1969) The uptake of oxygen by ammoniacal cobalt(II) solutions. *J. Am. Chem. Soc.* 91, 1325–1329.

(32) Michailidis, M. S., and Martin, R. B. (1969) Oxygenation and oxidation of cobalt(II) chelates of amines, amino acids, and dipeptides. *J. Am. Chem. Soc.* 91, 4683–4689.

(33) Miller, F., Simplicio, J., and Wilkins, R. G. (1969) The kinetics of the rapid interaction of some cobalt(II) chelates with oxygen. *J. Am. Chem. Soc.* 91, 1962–1967.

(34) Wilkins, R. G. (1971) Uptake of Oxygen by Cobalt (II) Complexes in Solution. *Adv. Chem. Ser.* 100, 111–134.

(35) Norkus, E., Vaskelis, A., Griguceviciene, A., Rozovskis, G., Reklaitis, J., and Norkus, P. (2001) Oxidation of cobalt(II) with air oxygen in aqueous ethylenediamine solutions. *Transition Met. Chem. (Dordrecht, Neth.)* 26, 465–472.